Published November 21, 2011

Crumbs regulates rhodopsin transport by interacting with and stabilizing myosin V

Shirin Meher Pocha,[1] Anna Shevchenko,[2] and Elisabeth Knust[1]

[1]Max Planck Institute of Molecular Cell Biology and Genetics, 01307 Dresden, Germany
[2]Mass Spectrometry Service Facility, Max Planck Institute of Molecular Cell Biology and Genetics, 01307 Dresden, Germany

The evolutionarily conserved Crumbs (Crb) complex is crucial for photoreceptor morphogenesis and homeostasis. Loss of Crb results in light-dependent retinal degeneration, which is prevented by feeding mutant flies carotenoid-deficient medium. This suggests a defect in rhodopsin 1 (Rh1) processing, transport, and/or signaling, causing degeneration; however, the molecular mechanism of this remained elusive. In this paper, we show that myosin V (MyoV) coimmunoprecipitated with the Crb complex and that loss of *crb* led to severe reduction in MyoV levels, which could be rescued by proteasomal inhibition. Loss of MyoV in *crb* mutant photoreceptors was accompanied by defective transport of the MyoV cargo Rh1 to the light-sensing organelle, the rhabdomere. This resulted in an age-dependent accumulation of Rh1 in the photoreceptor cell (PRC) body, a well-documented trigger of degeneration. We conclude that Crb protects against degeneration by interacting with and stabilizing MyoV, thereby ensuring correct Rh1 trafficking. Our data provide, for the first time, a molecular mechanism for the light-dependent degeneration of PRCs observed in *crb* mutant retinas.

Introduction

The transmembrane protein Crumbs (Crb) plays a crucial role in regulating photoreceptor cell (PRC) morphogenesis (Izaddoost et al., 2002; Pellikka et al., 2002) and in protecting PRCs from light-dependent degeneration (Johnson et al., 2002), the latter function being conserved between all core members of the Crb complex. Crb was first identified as an apical determinant in *Drosophila melanogaster* embryonic epithelia, where it is required for the maintenance of apicobasal polarity (Tepass et al., 1990; Wodarz et al., 1993, 1995; Tepass and Knust, 1993; Grawe et al., 1996; Tepass, 1996). The highly conserved intracellular domain of Crb recruits a core plasma membrane–associated protein scaffolding complex composed of the membrane-associated guanylate kinase protein Stardust (Sdt) and the PDZ domain–containing proteins *D*PatJ and *D*Lin7 (Bulgakova and Knust, 2009). In several tissues, stabilization and localization of all four components of the Crb complex members are interdependent (Richard et al., 2006a; Bachmann et al., 2008); for example, in adult *sdt* mutant PRCs, Crb protein levels are dramatically reduced, and *D*PatJ and *D*Lin7 are mislocalized (Bulgakova et al., 2008).

The role of Crb in the retina is evolutionarily conserved, as mutations in the human Crb homologue CRB1 result in retinitis pigmentosa and Leber's congenital amaurosis, both inherited retinopathies characterized by degeneration of PRCs and the gradual loss of vision (Richard et al., 2006b; den Hollander et al., 2008). Initial studies in flies showed that feeding larvae and flies a vitamin A (carotenoid)–depleted medium prevented the light-dependent degeneration of *crb* (Johnson et al., 2002), *sdt* (Berger et al., 2007), and *DLin7* mutant PRCs (Bachmann et al., 2008). In the absence of vitamin A, the levels of rhodopsin 1 (Rh1), the key light-sensing pigment in photoreceptors, is reduced by ∼97% (Nichols and Pak, 1985). These experiments indicated that degeneration in these mutants is somehow Rh1 dependent, but the molecular mechanisms were not known.

Rh1 is a crucial component of the *Drosophila* phototransduction cascade (Borst, 2009), and there is a vast body of literature documenting the degeneration that occurs upon disruption of its synthesis or maturation (Kumar and Ready, 1995; Rosenbaum et al., 2006; Wang and Montell, 2007; Griciuc et al., 2010;

Correspondence to Elisabeth Knust: knust@mpi-cbg.de; or Shirin Meher Pocha: pocha@mpi-cbg.de

Abbreviations used in this paper: Crb, Crumbs; dpe, day posteclosion; IF, immunofluorescence; IP, immunoprecipitate; MS, mass spectrometry; MyoV, myosin V; PRC, photoreceptor cell; Rh1, rhodopsin 1; Sdt, Stardust; UAS, upstream activating sequence; WB, Western blotting; WT, wild type.

The Rockefeller University Press $30.00
J. Cell Biol.
www.jcb.org/cgi/doi/10.1083/jcb.201105144

Published November 21, 2011

Wang et al., 2010), light-dependent internalization (Alloway et al., 2000; Kiselev et al., 2000; Satoh and Ready, 2005; Wang and Montell, 2007; Griciuc et al., 2010), or degradation (Chinchore et al., 2009). One major conclusion of all of these studies is that PRCs are exquisitely sensitive to perturbations in Rh1 and that any such impairment leads to retinal degeneration. Indeed, the pivotal role of Rh1 homeostasis in maintaining retinal integrity is also conserved in humans, as mutations in Rh1 alone account for >25% of autosomal dominant retinitis pigmentosa cases (Kennan et al., 2005).

To perform its function in the phototransduction cascade, mature Rh1 needs to be transported to the rhabdomere, the microvilli-based light-sensing organelle of the fly, analogous to the vertebrate photoreceptor outer segment. One of the proteins known to be crucial for this transport step is the actin-dependent motor protein myosin V (MyoV), which, in conjunction with Rab11 and dRip11, mediates the post-Golgi transport of Rh1 to the rhabdomere (Satoh et al., 2005; Li et al., 2007). In the absence of any of these proteins, Rh1 is retained within the cell body, and very little is seen entering the rhabdomere. MyoV is a member of the unconventional myosin family, which, unlike the conventional myosins, do not participate in filament formation and contractile force generation (Woolner and Bement, 2009). Instead, the unconventional myosins use their F-actin binding ability to transport organelles and secretory granules along F-actin tracks (for example, pigment granules in *Xenopus laevis* melanophores by myosin 5; Rodionov et al., 1998; Rogers and Gelfand, 1998). In addition, the unconventional myosins have recently been shown to be involved in a range of activities such as dynamic membrane tethering of endosomes and membrane-associated proteins, the organization of microtubule and actin-based structures, and the retrograde flow of F-actin in filopodia, microvilli, and stereocilia (Woolner and Bement, 2009).

Early studies in *Drosophila* embryos identified key domains in Crb that are vital for its function. The intracellular domain of Crb is crucial for its role in maintaining embryonic epithelial polarity, as a transgene encoding a truncated Crb protein lacking the extracellular domain is sufficient to suppress the embryonic *crb* mutant phenotypes to the same extent as full-length Crb (Wodarz et al., 1995). Interestingly, the ability of the truncated transgene to rescue requires the PDZ-interacting motif present at the very C terminus of Crb (Klebes and Knust, 2000). Therefore, the function of Crb in the embryo is dependent on its ability to interact with the cytosolic components of the Crb complex and is independent of the extracellular domain. The case is somewhat more complex in the eye, as two different mutant phenotypes are observed. As for embryonic epithelia, to rescue the morphological defects observed in the *crb* mutant retinas, the extracellular domain appears dispensable (Richard et al., 2009). On the contrary, rescue of the light-dependent degeneration observed in the absence of Crb requires the extracellular domain (Johnson et al., 2002). Indeed, the importance of the extracellular domain in preventing retinal degeneration seems to be conserved, as the vast majority of the mapped CRB1 mutations (including amino acid substitutions and in-frame deletions) that lead to retinopathies lie within the extracellular domain (den Hollander et al., 2004). These studies show that Crb performs its different functions through different domains and therefore most likely through different molecular mechanisms.

Results

MyoV interacts with the Crb complex

We reasoned that identification of novel interaction partners of Crb and the Crb complex would provide clues to understand the molecular mechanisms behind the light-dependent degeneration that occurs in the absence of any member of the Crb complex. To identify novel interactors, we used antibodies raised against different members of the Crb complex in an attempt to immunoprecipitate (IP) the entire complex and proteins associated with it. When *Drosophila* head lysate was incubated with antibodies raised against *D*PatJ or Sdt, we were able to coIP the other members of the complex (Fig. 1 A). Mass spectroscopic analysis of both IPs and a negative control IP using normal rabbit IgG confirmed that all Crb complex members were present in Sdt and *D*PatJ IPs, demonstrating the specificity of the IPs (Fig. 1 B). In addition, several putative interactors were coprecipitated. One potential interactor with an established role in the retina was the unconventional myosin MyoV. The mass spectroscopy analysis was verified by Western blotting (WB; Fig. 1 A), which confirmed that MyoV specifically coIPs with both Sdt and *D*PatJ, thus demonstrating that the Crb complex can interact with MyoV.

MyoV is dramatically reduced and partially mislocalized in Crb mutant retinas

To investigate the effect that loss of the Crb complex might have on MyoV, we induced the formation of mosaic eyes containing large *crb* mutant clones, using the functionally null mutant crb^{11A22}. Analysis of the protein levels of these adult retinas by WB revealed a marked reduction of MyoV protein in the absence of Crb protein (Fig. 1 C). Loss of MyoV protein was reproducible, and quantification by densitometry indicated that only ∼10% of MyoV protein remains in crb^{11A22} retinas when compared with wild-type (WT) levels (Fig. 1 D). These data suggest that Crb is required for the stabilization of MyoV in PRCs.

Consistent with published data (Li et al., 2007), Crb still localizes to the stalk membrane in MyoV mutant tissue (Fig. S1 A); therefore, MyoV is not required to transport Crb or members of the Crb complex to the apical membrane. A previous study into the role of MyoV in *Drosophila* PRCs showed that endogenous MyoV localizes to the rhabdomere base, an area abutting the stalk membrane and previously identified as the site of the rhabdomere terminal web, an actin-rich structure that protrudes from the rhabdomere into the cell body (Fig. 1 E; Li et al., 2007; Xia and Ready, 2011). To identify the localization of the remaining MyoV in *crb* mutant photoreceptors, we generated small clones of crb^{11A22} in the retina, allowing us to image mutant and WT tissue adjacent to one another. Staining such retinal sections (from 2–4-d-old adult flies) for MyoV confirms what we observe in the Western blot data, as very little signal can be detected in the mutant tissue (Fig. 2 A). The remaining MyoV localizes to the rhabdomere base and sometimes to the stalk membrane (Fig. 2 A, arrowheads), the latter being seldom, if ever, observed in WT tissue.

Published November 21, 2011

The actin terminal web is thought to provide the tracks along which MyoV transports its Rh1 payload. Therefore, we tested the integrity of this structure in *crb* mutant tissue to ensure that the loss of MyoV we observed is not a secondary effect caused by a loss of the actin terminal web. To test this, we expressed the F-actin–binding domain of moesin in a crb^{11A22} small clone background (Fig. S2). Despite the mosaic expression of the transgene, using this method, we could show that the F-actin tracks at the base of the rhabdomere were present in both WT and crb^{11A22} photoreceptors (Fig. S2, arrows). Therefore, we are confident that the loss of MyoV in crb^{11A22} tissue is not a result of morphological defects in the rhabdomere terminal web.

The finding that the residual MyoV is partially mislocalized led us to ask whether the Crb complex is required not only for protein stability but also for restricting MyoV to the rhabdomere base, preventing it from spreading to the stalk region of the apical membrane. To investigate this, we overexpressed a GFP-tagged MyoV (generated previously and shown to be functional; Krauss et al., 2009) in a crb^{11A22} small clone background. Overexpression of upstream activating sequence (UAS)–MyoV-GFP using *Rh1*-Gal4 drives expression of the transgene in the outer photoreceptors (R1–6) only. Most interestingly, staining for GFP (to detect the transgene-encoded protein only) or for MyoV (to detect both transgene-encoded and endogenous protein) showed that in otherwise WT PRCs, MyoV-GFP was well expressed (compare cells marked with arrows in Fig. 2 A with Fig. 2 C). However, in crb^{11A22} clones, the levels of MyoV-GFP and endogenous MyoV were dramatically reduced (Fig. 2, B and C). This reduction is similar to that seen when *crb* mutant eyes are stained for endogenous MyoV (Fig. 2 A). This suggests that the mechanism by which the Crb complex is controlling MyoV stability is tight enough to reduce MyoV protein levels even upon overexpression. In addition, these data rule out the possibility that Crb is directly controlling MyoV gene expression, as the MyoV-GFP is expressed under the control of an exogenous promoter.

MyoV is degraded by the proteasome in *crb* mutant photoreceptors

To investigate the cause of MyoV loss observed in *crb* mutant photoreceptors, we aimed to prevent the loss of MyoV by overexpression of a dominant-negative proteasome subunit Pros26^{1}2B (Belote and Fortier, 2002). This resulted in a marked increase in MyoV staining (compare Fig. 2 A with Fig. 2 D). Quantification of MyoV fluorescence (normalized to WT MyoV fluorescence per ommatidium, as described in Materials and methods) showed that the reduction of MyoV seen in *crb* mutant photoreceptors is rescued to ∼80% of that seen in WT ommatidia upon proteasome inhibition in comparison with ∼50% in the absence of proteasomal inhibition (Fig. 2 E). These data suggest that *crb* stabilizes MyoV protein by protecting it from degradation by the proteasome.

In addition, from this experiment, we can assess the localization of the rescued MyoV in the absence of Crb. Although MyoV does accumulate apically, it does not adopt the regular crescent shape seen in WT tissue and appears in large clumps rather than localizing to the entire rhabdomere base (Fig. 2 D).

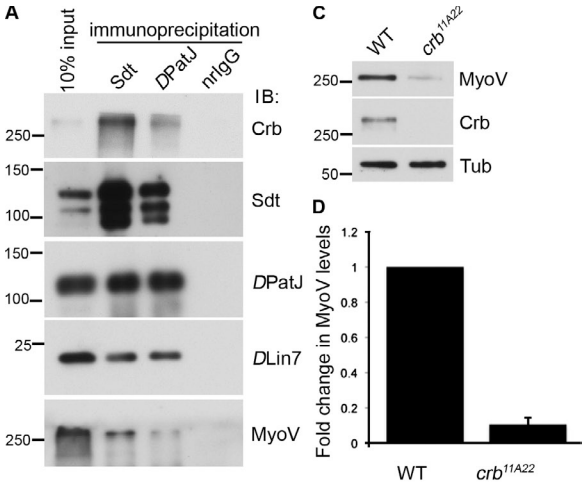

B

Protein	Number of unique peptides detected in IP		
	Sdt	*D*PatJ	nrIgG
Crumbs	11	11	-
Sdt	50	41	-
*D*PatJ	57	47	-
*D*Lin7	19	16	-
MyoV	6	3	-

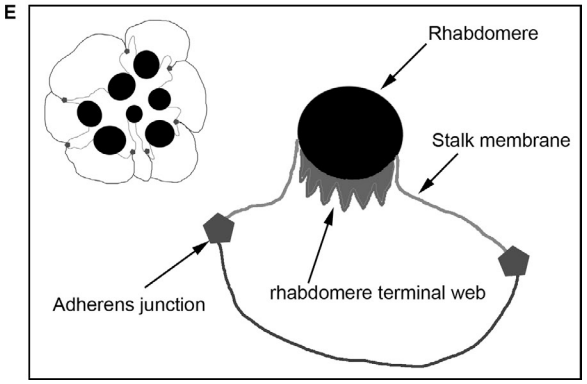

Figure 1. **The Crb complex interacts with MyoV.** (A) IPs from adult *Drosophila* heads using Sdt, *D*PatJ, or normal rabbit IgG (nrIgG) probed for members of the Crb complex and MyoV. The markers shown are for molecular masses in kilodaltons. IB, immunoblot. (B) MS data showing numbers of unique peptides of Crb complex members and MyoV (isoforms A and B) detected in IPs using Sdt, *D*PatJ, and normal rabbit IgG antibodies. (C) Western blots from whole-cell lysates of WT retinas and retinas harboring large clones of crb^{11A22}. Tubulin (Tub) is used as a loading control. (A and C) The markers shown are for molecular masses in kilodaltons. (D) Quantification of three independent experiments, as shown in C. Error bars represent mean ± SD. (E) Schematic of the stereotypical arrangement of photoreceptors in one ommatidium and a single photoreceptor.

Therefore, it appears that Crb is not directly responsible for the apical localization of MyoV.

MyoV fails to accumulate apically in *crb* mutant late pupal photoreceptors

To further analyze the functional interaction between MyoV and Crb, we studied earlier stages of retinal development (schematically represented in Fig. 3 A). At early pupal stages, around 30–40% pupal development, we observed that MyoV distributed evenly throughout the cell, not accumulating at any particular

Published November 21, 2011

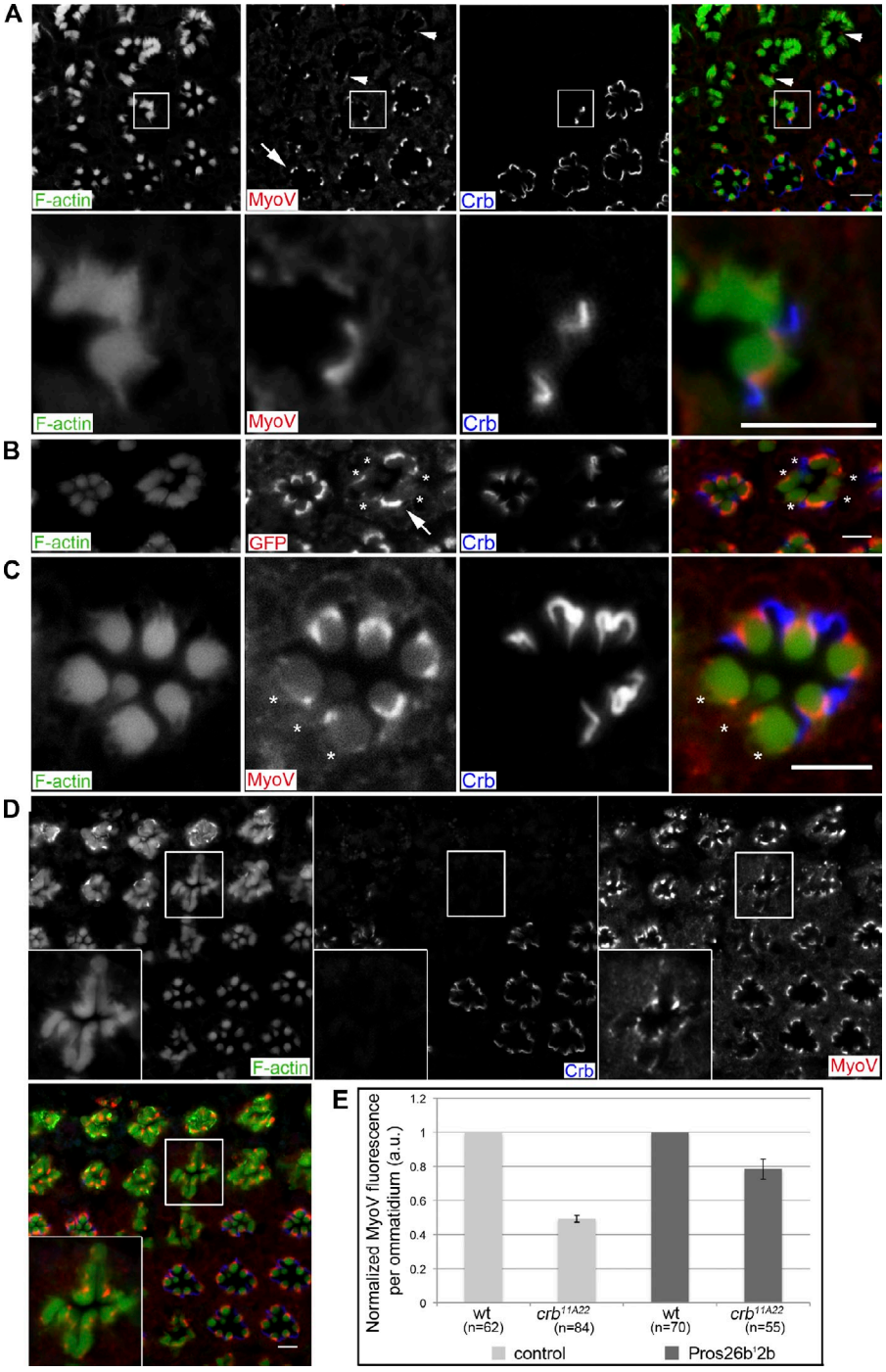

Figure 2. **MyoV is reduced and mislocalized in Crb mutant photoreceptors.** (A) Section through an adult retina harboring clones of *crb*^{11A22} tissue (identified by loss of Crb staining) stained for Crb, MyoV, and F-actin (to mark rhabdomeres). Arrowheads identify MyoV staining at the stalk membrane. White boxes are shown at higher magnifications in the bottom row. The arrow highlights WT MyoV staining to be compared with that in B. (B) Section through an adult retina harboring clones of *crb*^{11A22} (indicated by asterisks) and expressing MyoVGFP under the control of the Rh1 driver (expressed in outer photoreceptors only). Stained for GFP, Crb, and F-actin (to mark rhabdomeres). The arrow highlights overexpression of MyoV, including increased cytoplasmic staining when compared with that in A. (C) Section through an adult retina harboring clones of *crb*^{11A22} (indicated by asterisks) and expressing MyoVGFP under the control of an Rh1 driver (expressed in outer photoreceptors only). Stained for MyoV, Crb, and F-actin (to mark rhabdomeres). (D) Section through an adult retina harboring clones of *crb*^{11A22} and expressing Pros26^{1}2B under the control of an Rh1 driver (expressed in outer photoreceptors only). Stained for MyoV, Crb, and F-actin (to mark rhabdomeres). Boxed areas are enlarged in the insets. (A–D) Bars, 5 µm. (E) Quantification of MyoV fluorescence WT and of *crb*^{11A22} ommatidia in the presence of absence of Pros26^{1}2B expression. *n* indicates the number of ommatidia analyzed; error bars show SD (for more details, see Materials and methods). a.u., arbitrary unit.

subcellular location (Fig. 3 B). This MyoV distribution is unperturbed in early pupal *crb*^{11A22} mutant PRCs (Fig. 3 B, circled areas), suggesting that at early stages, before rhabdomere elongation, MyoV localization and levels are not Crb dependent. Expression of Rh1 starts at ∼70% pupal development (Satoh et al., 2005); therefore, if the steady-state localization of MyoV at the rhabdomere base correlates with its role in Rh1 transport, such localization would only develop at late pupal stages. Indeed, in pharate adults (around 80–90% pupal development), MyoV starts to accumulate apically (Fig. 3 C). Interestingly, at this stage, MyoV decorates not only the rhabdomere base but is also seen at the stalk membrane, colocalizing with Crb to a small extent (Fig. 3 C, arrows). In *crb*^{11A22} mutant photoreceptors, the apical accumulation is dramatically reduced (Fig. 3 C). From these data, we conclude that at early pupal stages, MyoV is independent of Crb, whereas at later stages, Crb is required for MyoV apical accumulation.

crb^{8F105} mutants partially maintain MyoV levels and localization

To further investigate the interaction between the Crb complex and MyoV, we analyzed a weaker *crb* allele, *crb*^{8F105}, which contains a stop in the cytoplasmic domain and results in the production of a truncated protein lacking the C-terminal 23

Published November 21, 2011

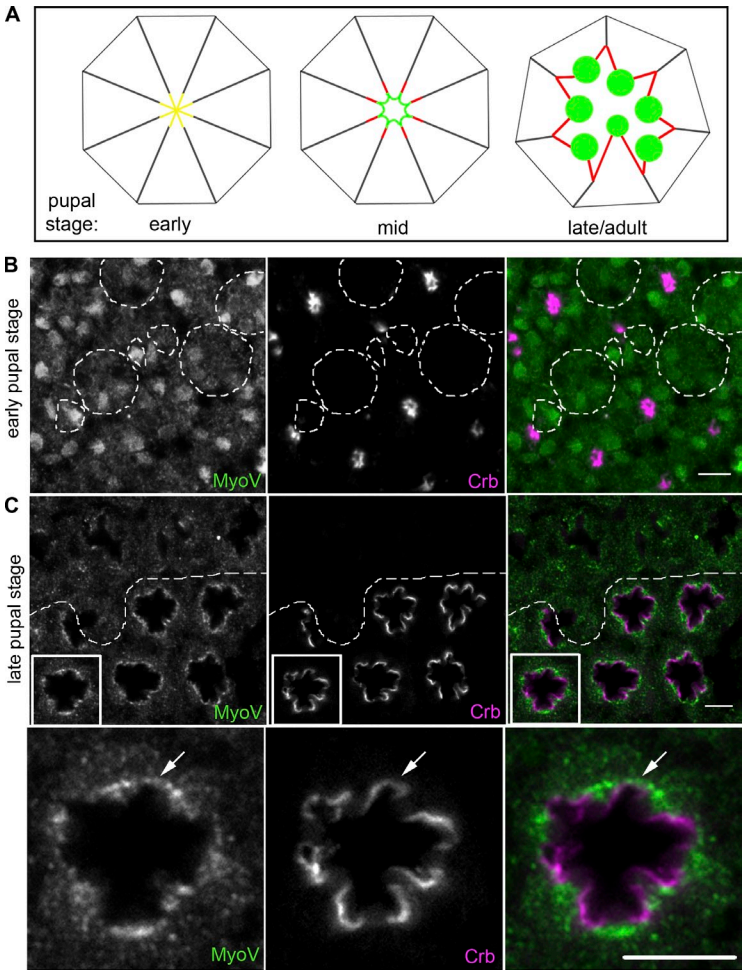

Figure 3. **MyoV fails to accumulate apically in late pupal stages in the absence of Crb.** (A) Schematic of the development of one ommatidium from early pupal stages to adulthood. Crb-decorated membrane is shown in red, and actin-rich areas, which will form or form the rhabdomere, are shown in green. Note that at early stages, Crb decorates the entire apical membrane and hence colocalizes with actin. (B and C) Early and late pupal stage retinas containing crb^{11A22} clones stained for MyoV and Crb. Mutant tissues are outlined with dashed white lines. White boxes in C are magnified in the bottom row. Arrows indicate MyoV staining at the stalk membrane. Bars, 5 µm.

amino acids and, thus, the PDZ-binding motif (Wodarz et al., 1993). This truncated protein localizes to the stalk membrane and ectopically to the outermost membranes of the rhabdomere (Fig. S3 B). crb^{8F105} mutant photoreceptors display morphological defects, which are slightly less severe than those seen in crb^{11A22} mutants. Interestingly, despite the absence of the Sdt-binding ERLI motif in the truncated protein, crb^{8F105} mutant photoreceptors retain low levels of Sdt protein, which is, however, mislocalized (Fig. S3, A and B). Most importantly, crb^{8F105} mutant photoreceptors do not undergo light-dependent degeneration (Johnson et al., 2002). The localization of MyoV in crb^{8F105} mutant photoreceptors is similar to that seen in WT tissue (Fig. 4 A), showing enrichment at the rhabdomere base (Fig. 4 A, arrows) and also an accumulation in cytoplasmic puncta within the cell body. This partial maintenance of MyoV localization in crb^{8F105} mutant PRCs is concomitant with increased MyoV protein in crb^{8F105} mutants compared with crb^{11A22} mutants (Fig. 4 B) but still reduced levels compared with WT PRCs. The latter could be explained by the fact that truncated Crb protein is expressed to a slightly lower level than the WT Crb protein (Fig. 4 B). These data suggest that the stability of MyoV does not depend on an intact Crb complex; however, the presence of residual levels of Sdt in the crb^{8F105} mutants leaves open the possibility that Sdt is able to stabilize MyoV in these photoreceptors, despite being mislocalized.

Expression of Crb in S2R+ cells in the absence of Sdt recruits MyoV-GFP to the plasma membrane

To further investigate the possibility that Crb itself can interact with MyoV, we took advantage of the *Drosophila* S2R+ cell line that does not express endogenous *crb* or *sdt* (Fig. S4 A). This allowed us to express *MyoV-GFP* with and without Crb in the system. Importantly, Crb expression in S2R+ cells does not result in the expression of Sdt (Fig. S4 B). When expressed alone, MyoV-GFP localizes to puncta distributed evenly throughout the cell (Fig. 4 C). Strikingly, upon coexpression with Crb, MyoV-GFP is recruited to the plasma membrane, where it colocalizes with Crb (Fig. 4, D and E). The ability of Crb to recruit MyoV-GFP to the plasma membrane in the absence of Sdt strongly argues that the interaction with MyoV is not depended on Crb acting as part of the Crb complex but rather on Crb itself.

The recruitment of MyoV-GFP to the plasma membrane in S2R+ cells requires only the membrane-spanning region and first 14 amino acids of the intracellular domain of Crb

To further characterize the interaction between Crb and MyoV, we used the S2R+ system to express *MyoV-GFP* with various Crb truncations. First, to confirm the data acquired using the

Published November 21, 2011

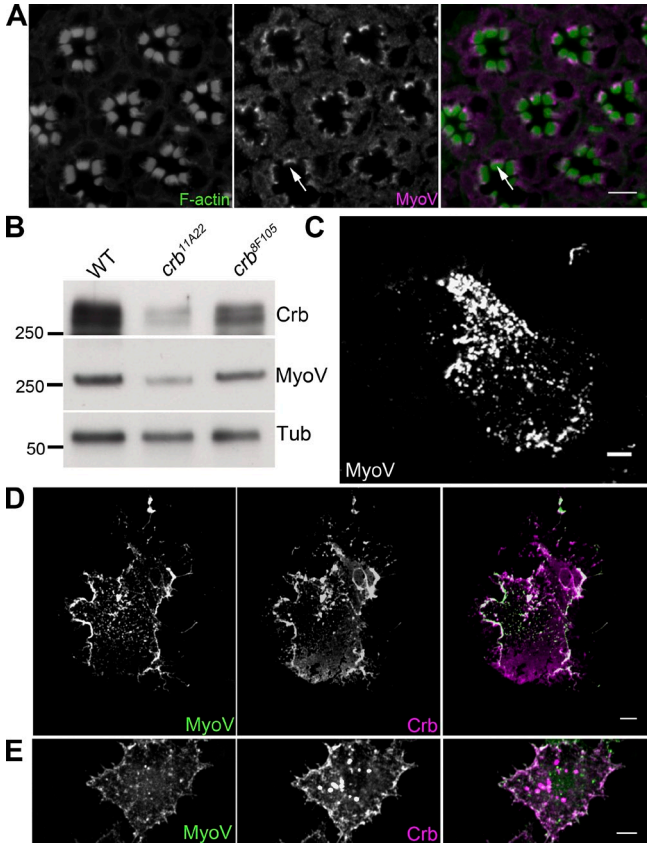

Figure 4. **MyoV stabilization does not require an intact Crb complex.** (A) Section through an adult retina harboring *crb*^{8F105} large clones stained for MyoV and F-actin. Arrows highlight MyoV enrichment at the base of the rhabdomere, as seen in WT photoreceptors. (B) Western blots from whole-cell lysates of WT retinas and retinas harboring large clones of *crb*^{11A22} or *crb*^{8F105}. Tubulin (Tub) is used as a loading control. The markers shown are for molecular masses in kilodaltons. (C) An S2R+ cell expressing MyoV-GFP and plated on concanavalin A shows a punctate distribution throughout the cell. (D and E) S2R+ cells coexpressing MyoV-GFP and Crb and plated on concanavalin A show recruitment of MyoV-GFP to the plasma membrane, where it colocalizes with Crb. Bars, 5 µm.

crb^{8F105} mutant, we expressed the truncated form of Crb found in this mutant together with MyoV-GFP. The truncated Crb^{8F105} protein localizes to the plasma membrane of S2R+ cells and recruits MyoV-GFP in a similar manner to full-length Crb (Compare Fig. 5 [A and B] with Fig. 4 [D and E]). This finding further strengthens our conclusion that the interaction between Crb and MyoV does not require the cytosolic components of the Crb complex. To assess the role of the extracellular domain in this interaction, we then expressed Crb constructs that contain a myc tag and that do not contain the extracellular domain (referred to as Crb^{intramyc}) and a truncated version of this construct that lacks the ERLI motif (Crb$^{intramyc\Delta ERLI}$). Again, both of these proteins were able to recruit MyoV-GFP to the plasma membrane of S2R+ cells (Fig. 5, C and D), suggesting that the interaction between Crb and MyoV does not require the extracellular region of Crb. Furthermore, together with the Crb^{8F105} data, we can narrow down the interaction site between Crb and MyoV to the transmembrane-spanning region and the first 14 amino acids of the intracellular domain. As MyoV is a cytosolic protein, it therefore seems likely that the interaction is mediated by the first 14 amino acids of the cytosolic domain of Crb; however, as these experiments are performed in cells, we cannot rule out the possibility that there are other mediators of this interaction that could be membrane or cytosolic proteins.

In *Drosophila* PRCs, Crb overexpression does not lead to the mislocalization of MyoV

Although the results from the S2R+ experiments allowed us to narrow down the portion of Crb required for interaction with MyoV, they also showed that in this system, Crb could ectopically recruit MyoV to the plasma membrane. Despite the extremely simplified nature of the S2R+ system in comparison with PRCs and the fact that in *crb* mutant photoreceptors, the residual MyoV localization is predominantly WT, we tested whether or not Crb is capable of performing the same function in PRCs. Using *Rh1*-Gal4, we expressed either full-length Crb (Crb$^{Full\ length}$) or a construct of Crb in which the extracellular domain of Crb has been replaced by a Flag tag (Crb$^{Flag\ intra}$). Although both of these transgene-encoded proteins localize ectopically to the rhabdomere base and basolateral membranes, as previously described (Richard et al., 2009), neither is able to recruit MyoV to these sites (Fig. 5, E and F). Therefore, we conclude that the S2R+ experiments can be used only as a basic method to analyze the domains for the Crb–MyoV interaction and that the physiologically relevant role of this interaction in the adult photoreceptor is not one of recruitment/localization but rather of stabilization.

Rhodopsin transport is defective in *crb* mutant PRCs

As previously shown (Li et al., 2007), *MyoV* mutants exhibit defects in Rh1 transport to the rhabdomere (Fig. S1 A). Interestingly, this phenotype depended heavily on the *MyoV* allele used. Severe defects in Rh1 transport were only seen with null mutations, whereas hypomorphic alleles displayed normal steady-state Rh1 staining (Li et al., 2007). The authors concluded from this that only minimal MyoV activity is sufficient for Rh1 transport.

Therefore, we tested the localization of Rh1 in eyes containing *crb*^{11A22} small clones. The WT steady-state localization of Rh1 is light dependent; in the dark, it fills the entire rhabdomere, whereas upon light exposure, Rh1 is restricted to a crescent shape at the lower half of the rhabdomere (Satoh and Ready, 2005). Despite the enlarged rhabdomeres seen in *crb*^{11A22} photoreceptors, the normal crescent of Rh1 is still detectable (Fig. 6 A, arrows), suggesting that the residual MyoV present in *crb*^{11A22} cells is sufficient to transport Rh1. As staining of Rh1 in very young adult flies represents the steady state after very little exposure to the night/day cycling, we left *crb*^{11A22} mosaic–eyed flies in normal night/day conditions for 20 d posteclosion (dpe), reasoning that subtle defects in Rh1 transport might accumulate over time. In *crb*^{11A22} photoreceptors kept under these conditions, Rh1 staining shows an accumulation in large punctae in the cytoplasm (Fig. 6 B, arrowheads), which is seldom observed in neighboring WT tissue. The accumulation of Rh1 within PRC bodies is closely linked to degeneration (Satoh and Ready, 2005; Chinchore et al., 2009). Therefore, we tested whether

Published November 21, 2011

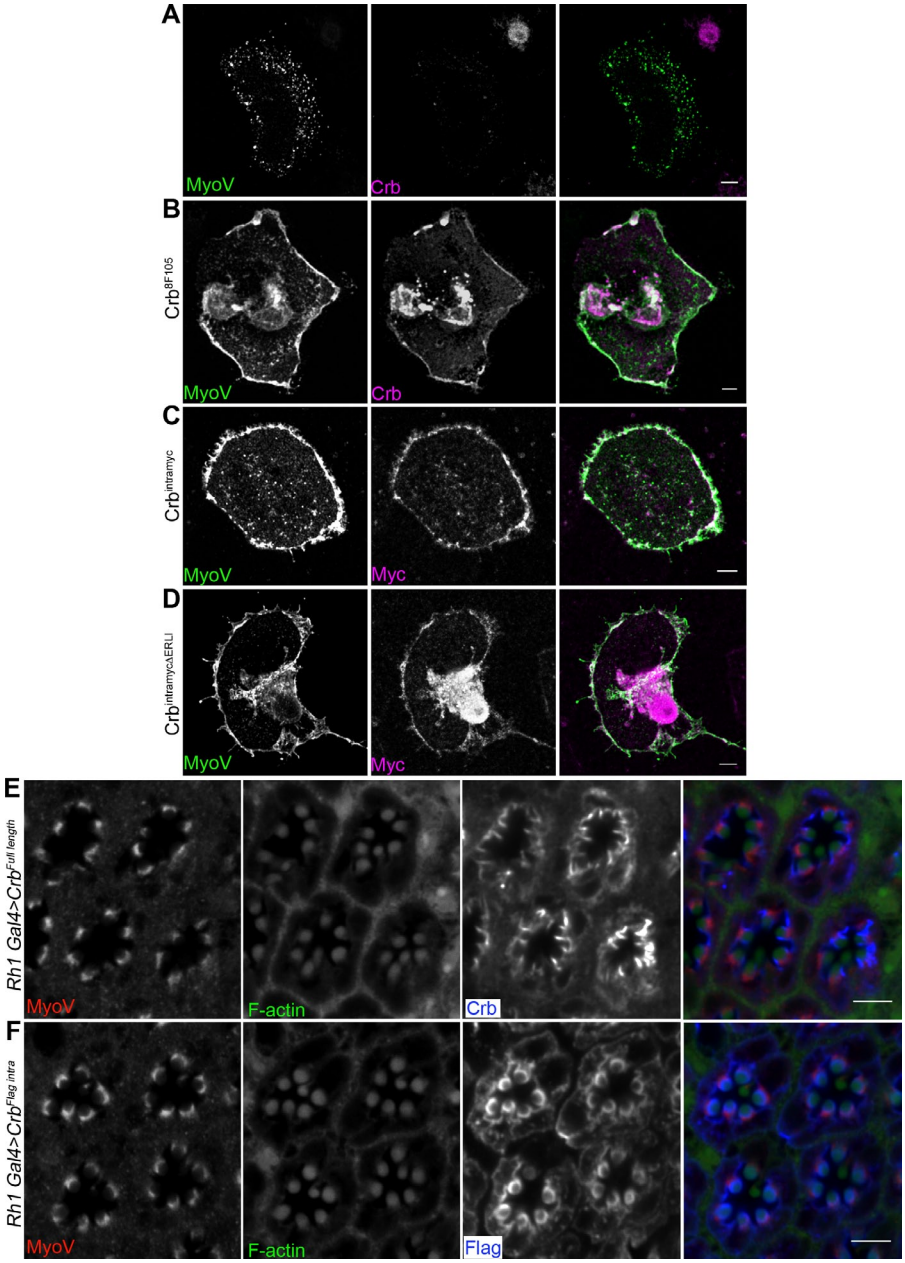

Figure 5. **The interaction between Crb and MyoV requires only the transmembrane-spanning and first 14 amino acids of the cytoplasmic domain.** (A and B) S2R+ cells transfected with MyoV-GFP and $Crb^{8F10.5}$ and plated on concanavalin A. A cell expressing MyoV-GFP only is shown in A as a control. (C and D) S2R+ cells coexpressing MyoV-GFP and $Crb^{intramyc}$ (C) or $Crb^{intramyc\Delta ERLI}$ (D) and plated on concanavalin A, showing some recruitment of MyoV-GFP to the plasma membrane, where it colocalizes with $Crb^{Myc\ intra}$. (E and F) Sections through adult retinas expressing $Crb^{Full\ length}$ (E) or $Crb^{Flag\ intra}$ (F) under the control of the Rh1 promoter, stained for MyoV, F-actin, and Crb (E) or Flag (F). Bars, 5 µm.

crb^{11A22} mutants show signs of degeneration at 20 dpe under normal night/day conditions. Electron micrographs of *crb*^{11A22} mutant PRCs at 3 dpe show no defect in the ultrastructure of the rhabdomeres; microvilli are intact and tightly packed, as in neighboring WT cells (Fig. 6 C). At 20 dpe, however, nearly all *crb*^{11A22} mutant ommatidia contain rhabdomeres that exhibit features of disintegration (Fig. 6 D); packing of microvilli is not as tight as in neighboring WT cells, and there is an increased loss of microvillar material into the interrhabdomeral space, which is rarely seen in WT rhabdomeres (Fig. 6 D) nor in w^- controls (Fig. S1 B). Together, these data indicate that *crb* mutant photoreceptors display subtle defects in Rh1 localization and, over time, start displaying signs of degeneration.

The accumulation of Rh1 within the cell body of 20-dpe *crb*^{11A22} mutant photoreceptors might be caused by defects in synthesis, transport to the rhabdomere, or recycling. As MyoV was shown to be required for the post-Golgi transport of Rh1 to the rhabdomere, we tested the role of *crb* in the movement of Rh1 through the secretory pathway using a pulse-chase assay that takes advantage of the highly complex Rh1 biogenesis (Satoh et al., 1997). Flies raised on carotenoid-free media synthesize little or no Rh1 protein, as the chromophore is absent. Feeding these animals with all-trans-retinal and maintaining them in the dark result in the production of Rh1 protein containing all-trans-retinal, which is retained within the ER. Exposure of these flies to a pulse of blue light isomerizes the chromophore to 11-cis-retinal, which allows Rh1 to be transported through the secretory pathway and into the rhabdomere (depicted schematically in Fig. 7 A; Satoh et al., 1997). Performing this assay on flies harboring *crb*^{11A22} retinal clones shows that at early time points 20 and 40 min after blue light pulse, there is little difference in the transport between the mutant and WT tissue (Fig. 7, B and C).

Published November 21, 2011

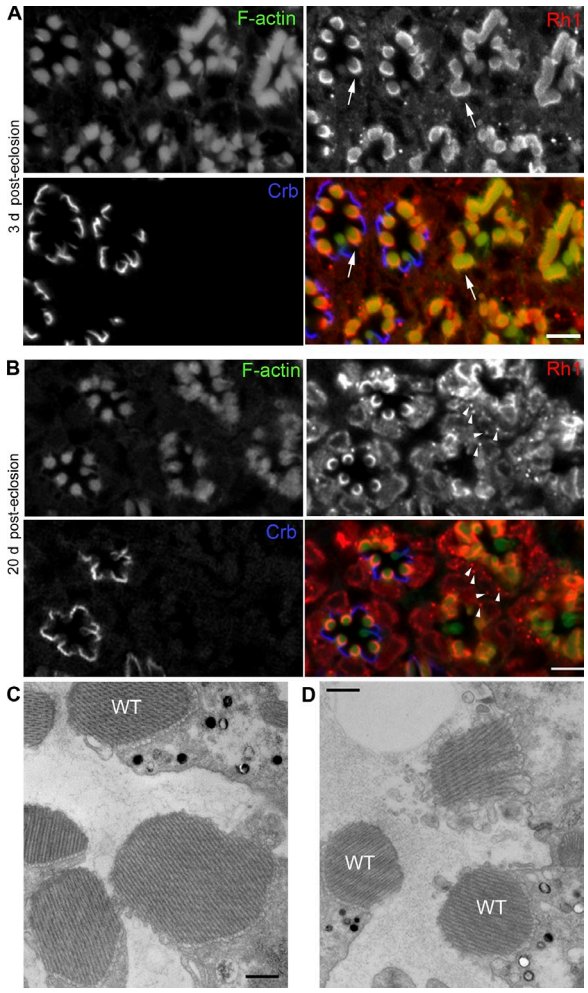

Figure 6. ***crb* mutant PRCs display age-dependent defects in Rh1 transport.** (A and B) Sections through adult retinas containing crb^{11A22} clones from flies that are 3 (A) and 20 (B) dpe, stained for Rh1, Crb, and F-actin. Arrows in A indicate the crescent of Rh1 observed after light exposure. Arrowheads in B denote the intracellular accumulation of Rh1 punctae. Bars, 5 µm. (C and D) Electron micrographs of retinas containing crb^{11A22} clones from 3-dpe (C) and 20-dpe (D) adult flies. WT photoreceptors are identifiable by the presence of pigment granules accumulating at the rhabdomere base. Bars, 500 nm.

However, at later stages 60, 80, and 120 min after pulse, there is a clear delay in transport to the rhabdomere in crb^{11A22} cells, with Rh1 remaining within the cell body of mutant photoreceptors when most has already reached the rhabdomere of WT cells (Fig. 6, B and C). This is consistent with the role of MyoV in post-Golgi transport of Rh1 to the rhabdomere, as early time points during which Rh1 is transported from ER to Golgi appear unaffected. Thus, we conclude that in the absence of *crb*, transport of Rh1 to the rhabdomere is delayed, and we propose that this is a result of the reduction of MyoV in these photoreceptors.

Discussion

The role of the Crb complex in polarity is well studied, but the mechanism behind its ability to prevent light-dependent retinal degeneration is poorly understood. Some insight into the latter came from studies reporting that feeding flies a vitamin A (carotenoid)–depleted medium prevented the light-dependent degeneration of *crb*, (Johnson et al., 2002), *sdt* (Berger et al., 2007), and *DLin7* mutant PRCs (Bachmann et al., 2008). These data suggested that degeneration in Crb complex mutants involves Rh1; however, the molecular mechanism behind this remained unknown. Here, we provide the missing link by showing that the Crb complex interacts with MyoV, an unconventional myosin, which has an established role in the transport of Rh1 to the rhabdomere. We show that MyoV levels are reduced by ∼90% in *crb* mutant retinas, which can be largely rescued by inhibition of the proteasome, and that Rh1 transport is defective in *crb* mutant PRCs. Therefore, we propose that the Crb complex protects against light-dependent degeneration by interacting with and maintaining MyoV levels, thereby ensuring proper Rh1 transport to the rhabdomere.

Blocking proteasome activity also allowed us to assess the localization of MyoV in the absence of Crb. We observed apical localization of MyoV; however, rather than adopting the WT localization that spans the entire rhabdomere base, the rescued MyoV was seen in large clumps, which only partially covered the base of the rhabdomere. The steady-state WT localization of MyoV reflects its role in transporting Rh1 from the cell body to the rhabdomere base. Therefore, these large accumulations may suggest that some level of MyoV degradation is also important for maintaining efficient transport by the total pool of MyoV. Thus, the levels of MyoV and its ability to transport Rh1 to the rhabdomere base may depend on external cues (e.g., light), which alter the balance between stabilization and degradation.

We show that IPs of both Sdt and *D*PatJ contain the respective other members of the Crb complex and that together with these, MyoV is precipitated specifically. The strong reduction in MyoV protein we see in *crb* mutant photoreceptors raises the question of whether stability of MyoV is dependent on Crb itself or on the integrity of the Crb complex. As loss of Crb results in the loss of Sdt (Fig. S3; Bachmann et al., 2008) and the delocalization of *D*PatJ and *D*Lin7 (Richard et al., 2006a; Bachmann et al., 2008), the data obtained using crb^{11A22} mutants can be used to analyze the role of the Crb complex. Data obtained from crb^{8F105} mutants, however, show that the integrity of the Crb complex is not required for the *crb*-dependent stabilization of MyoV. This was further supported by experiments in S2R+ cells that showed Crb alone, in the absence of Sdt, can recruit MyoV-GFP to the plasma membrane, suggesting that the interaction we observe between Crb and MyoV is not mediated by any of the other core components of the Crb complex. As we detected the interaction by IP, the possibility remains that the interaction between Crb and MyoV is mediated by another still unknown protein.

Interestingly, loss of MyoV in crb^{11A22} mutants cannot be overcome by overexpression of a MyoV transgene, which is expressed under the control of an exogenous system, the UAS/Gal4 system. This demonstrates that Crb is required to maintain MyoV stability posttranscriptionally. We investigated this further by inhibiting proteasomal degradation and observed a marked increase of MyoV staining in *crb* mutant photoreceptors compared with controls. These findings support our previous conclusion that the

Published November 21, 2011

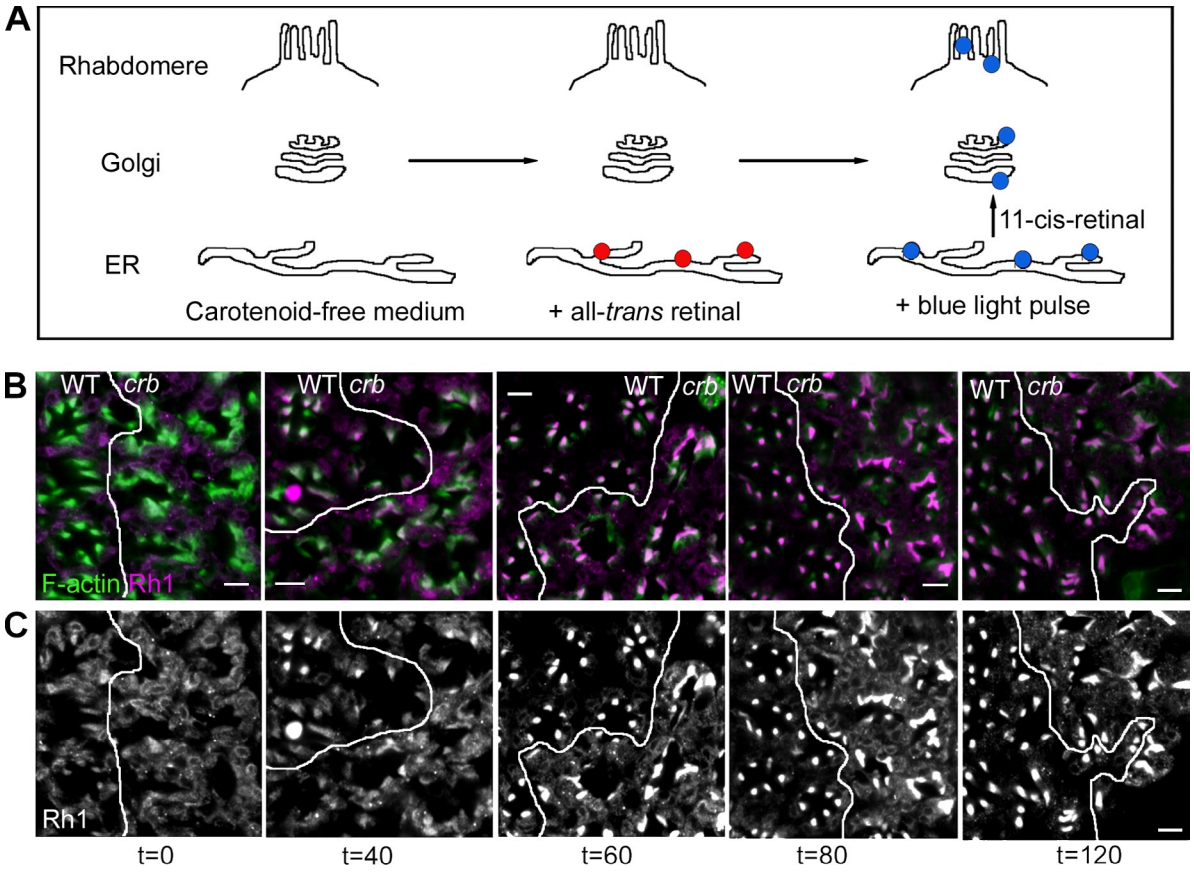

Figure 7. **Crb mutant PRCs display slower Rh1 transport kinetics.** (A) Schematic of the Rh1 pulse-chase experiment. Red dots symbolize immature Rh1 containing all-trans-retinal. Blue dots symbolize mature Rh1 containing 11-cis-retinal (for a detailed description, see Results and Materials and methods). (B and C) Rh1 pulse-chase experiment. Sections through adult retinas containing crb^{11A22} clones from flies that were fed on carotenoid-free medium from egg to adult, given all-trans-retinal for 2 d in the dark, and then pulsed with CFP-filtered light for 10 min and returned to the dark for the times indicated. Sections were stained for Rh1 and F-actin. Borders between WT and crb^{11A22} (*crb*) tissue are outlined in white. The structure of the eye is not as well preserved as those in Fig. 5 A because the flies are fixed whole to avoid exposure to light before fixation. Bars, 5 µm.

interaction between Crb and MyoV is stabilizing the latter by protecting it from degradation by the proteasome.

crb is known to have two main functions in the eye, one during development of the retina to ensure correct morphogenesis of the PRCs (Izaddoost et al., 2002; Pellikka et al., 2002) and the other to prevent degeneration of the adult eye in constant light (Johnson et al., 2002). Here, we show that MyoV does not show a polarized distribution at early pupal stages nor is its localization perturbed by loss of Crb in early stages, the time at which morphogenetic defects in *crb* mutants start (Izaddoost et al., 2002; Pellikka et al., 2002), suggesting that the interaction between Crb and MyoV is not required for proper morphogenesis to occur. This is supported by reports that MyoV-null mutant adults display only mild morphological defects, which are distinct from those observed in *crb* mutants (Li et al., 2007; Satoh et al., 2008).

The finding that MyoV fails to start accumulating apically in *crb* mutant cells during late pupal stages after Rh1 expression starts corroborates the conclusion that the Crb–MyoV interaction is required for the second role of Crb in the retina, preventing light-dependent degeneration. It is also plausible that the steady-state localization of MyoV seen in the adult is largely the result of its role in Rh1 transport to the rhabdomere, as MyoV is seen evenly distributed throughout the cell before Rh1 expression starts. This assumption is supported by published data showing that the localization of MyoV in the adult is light dependent (Satoh et al., 2008) and therefore reflects the status of Rh1 activation and transport. Fittingly, the apical accumulation of MyoV at later pupal stages coincides with increased MyoV staining and increased colocalization of MyoV with Crb.

We tested the effect that loss of Crb has on Rh1 and demonstrated that in normal 12-h light/12-h dark conditions, defects in Rh1 staining are only seen in old flies. This is suggestive of a subtle defect in Rh1 transport that is only visible at steady state if allowed to accumulate over time or if the system is under stress (i.e., constant light). As it was reported that only minimal MyoV activity is required for proper Rh1 localization (Li et al., 2007), it is probable that the remaining 10% of MyoV seen in *crb* mutants is sufficient for Rh1 transport in young flies, but, over time, the effect of this deficiency accumulates, resulting in the retention of Rh1-positive punctae in the cell body. Together with our results from the Rh1 pulse-chase assay, we conclude that in *crb* mutant tissue, Rh1 transport to the rhabdomere is delayed and that the cumulative effect of this delayed transport leads to the accumulation of Rh1 within the cell body, which is associated with a gradual deterioration of the rhabdomeres.

Published November 21, 2011

Previous findings have shown that Crb-mediated protection against light-dependent retinal degeneration is not solely dependent on the ability of Crb to assemble and integrate into the Crb complex (Johnson et al., 2002). Photoreceptors of crb^{8F105} mutants, which express a Crb protein lacking the Sdt-interacting ERLI motif, do not undergo light-dependent degeneration. This observation is in agreement with the findings we present here that MyoV is retained in Crb^{8F105} mutant photoreceptors. In addition, overexpression of a Crb transgene encoding the transmembrane and intracellular domains was not able to rescue the light-dependent degeneration observed in crb^{11A22} mutants (Johnson et al., 2002). Interestingly, this membrane-tethered intracellular domain–encoding transgene does rescue the morphogenetic defects observed in both crb^{8F105} and crb^{11A22} mutants (Richard et al., 2009). Therefore, the two roles of Crb in the retina—photoreceptor morphogenesis and maintenance—appear to occur through distinct mechanisms. Correct morphogenesis seems to necessitate the assembly of the Crb complex through the Crb ERLI motif. In contrast, Crb-mediated protection against light-dependent degeneration and stabilization of MyoV does not require an intact Crb complex. How do these finding correlate with reports of light-dependent retinal degeneration in other members of the Crb complex? We propose that in *sdt* and *DPatJ* mutants, it is the concomitant loss of Crb that is responsible for the degeneration phenotype rather than the loss of an intact Crb complex itself.

The absence of endogenous Crb and Sdt from S2R+ cells made them particularly useful to identify the regions of Crb required for its interaction with MyoV, which we determined to include the membrane-spanning and first 14 amino acids of the cytoplasmic domain. However, the readout for this interaction—the recruitment of MyoV-GFP to the plasma membrane—may not reflect the purpose of this interaction in vivo, particularly considering the highly polarized and functionally specialized nature of PRC. Indeed, the finding that the majority of the residual MyoV in *crb* mutant photoreceptors localizes to the rhabdomere base suggests that in photoreceptors, the role of the Crb–MyoV interaction is primarily to stabilize MyoV and not to recruit it to the rhabdomere base. In addition, the ability of Crb lacking the extracellular domain to recruit MyoV to the plasma membrane of S2R+ cells but not to rescue light-dependent degeneration suggests that S2R+ cells lack many qualities (morphology, protein expression, and functionality) of PRCs. Considering the requirement of the extracellular domain (discussed in the Introduction), it is possible that in the context of a light-sensing photoreceptor, Crb responds to a stimulus that is transmitted via the extracellular domain, which then initiates the interaction with and/or the stabilization of MyoV. This hypothesis is an intriguing one, as the only function of Crb that requires its extracellular domain is its role in preventing light-dependent degeneration, and, to date, no known partner of the extracellular domain has been identified.

We propose a model in which the interaction between Crb and MyoV stabilizes the latter, maintaining a complete Rh1 transport cycle. In *crb* mutants, this cycle is slowed down at the MyoV-dependent stage of delivery to the rhabdomere. Whereas in normal light/dark conditions the effect of this is minimal, upon exposure to constant light, Rh1 accumulates in the cell body, suggesting that the rate of removal from the rhabdomere (as a result of constant activation) exceeds the rate of delivery to the rhabdomere. As previously discussed, photoreceptors are extremely sensitive to perturbations in the phototransduction cascade, and it has been well documented that mutations that affect the synthesis, delivery, and recycling of Rh1 lead to degeneration. Together with previously published data showing the rescue of Crb-dependent retinal degeneration in the absence of vitamin A, this strongly supports our model that the accumulation of Rh1 in the cell body as a result of a deficiency of Rh1 transport in *crb* mutants leads to degeneration.

These data provide for the first time a molecular mechanism for the light-dependent degeneration observed in *crb* mutant animals. Recent findings that *myoVIIa* mutant mice display light-dependent degeneration as a result of defects in rod protein translocation (Peng et al., 2011) suggest that the efficient transport of opsins by myosins is crucial to prevent degeneration across species. Therefore, it will be intriguing to see whether the mechanism we identified here is conserved and whether human photoreceptors from patients with CRB1 mutations also display reduced myosin levels and delays in Rh1 transport.

Materials and methods

Drosophila genetics

Large *crb* mutant clones were generated by crossing male *FRT82B* crb^{11A22}*/TM6B* (Wodarz et al., 1995) or *FRT82B* crb^{8F105}*/TM6B* flies to *eyFLP;;FRT82Bcl(3)*w^+ virgins. Small clones were generated by crossing *yw eyFLP;;FRT82Bneo*$^+$$w^+$ virgins to *w;FRT82B* crb^{11A22}*/TM6B* or *FRT82B* crb^{8F105}*/TM6B* males. Crb overexpression was achieved by crossing *Rh1 Gal4* (Tabuchi et al., 2000) virgins to *UAS* $Crb^{Full\ length}$ (line $Crb^{wt\text{-}2e}$ was previously described in Wodarz et al. [1995]) or *UAS* $Crb^{Flag\ intra}$ (Richard et al., 2009) males. MyoV clones were generated using *yw hsFLP;FRT42B ubiGFP* virgins crossed to *w;FRT42BMyoV*^{Q105st} (a gift from D. Ready, Purdue University, West Lafayette, IN). Heat shock was performed on first instar larvae at 37°C for 2 h. *UASMyoVGFP/TM6B* was a gift from A. Ephrussi (European Molecular Biology Laboratory, Heidelberg, Germany; Krauss et al., 2009). *UASPros26*^{1}*2B* flies were obtained from the Bloomington Drosophila Stock Center at Indiana University.

Antibodies

Antibodies were used at the following concentrations for WB or immunofluorescence (IF): rat anti-Crb 2.8 (1:2,000; WB and IF; Tepass et al., 1990), rabbit anti-Sdt (1:1,000; WB; Berger et al., 2007), rat antitubulin (1:4,000; WB; AbD Serotec), rabbit anti-PatJ (1:3,000; WB; Richard et al., 2006a), rat anti-Lin7 (1:2,000; WB; Bachmann et al., 2004), rabbit anti-Rh1 (1:1,000; IF; a gift from D. Ready), rabbit anti-GFP (1:1,000; IF; Invitrogen), mouse anti-Myc (9E10 supernatant; 1:75; IF; Developmental Studies Hybridoma Bank), mouse anti-Flag (M2; 1:1,000; IF; Sigma-Aldrich), and normal rabbit IgG (Santa Cruz Biotechnology, Inc.). Rabbit anti-MyoV was generated as previously described (Li et al., 2007) and purified as described in Pocha and Cory (2009). In brief, rabbit antisera were raised against the peptide CGGEDIELPSHLNLDEFLTKI conjugated to keyhole limpet haemocyanin (Charles River). Serum from the final bleed was clarified by centrifugation at 25,000 *g* for 30 min, and the supernatant was supplemented with 1× TTBS (0.5 M NaCl, 20 mM Tris, pH 8.0, and 0.1% Tween 20). This was then purified using an affinity column containing the peptide coupled to epoxy–Sepharose 6B (GE Healthcare). Clarified serum was passed over the column twice, and then the column was washed with TTBS until the flow-through had an OD_{280} nm < 0.01. Antibodies were then eluted using 0.2 M glycine and neutralized with Tris-HCL, pH 8.0.

Immunoprecipitation

Drosophila heads were lysed in a homogenizer with the following lysis buffer: 50 mM Tris, pH 8, 0.5% Triton X-100, 130 mM NaCl, 1 µg/ml leupeptin, 250 µg/ml PefaBloc, 2 µg/ml aprotinin, and 1 µg/ml pepstatin.

Published November 21, 2011

The lysate was left on ice for 30 min and then clarified by centrifugation. 6 mg total protein was used per IP. Antibody was added to the lysate and incubated at 4°C rotating for 1 h. Then, 50 µl protein G agarose (GE Healthcare) per IP was added to the lysate antibody mixture and left to rotate again at 4°C for 3 h. The beads were then washed with lysis buffer six times and then boiled with loading buffer for 5 min at 105°C and analyzed by conventional SDS-PAGE. Mass spectrometry (MS) was then performed as described in the next section.

Preparation of samples for MS

After protein separation, SDS gels were stained with Coomassie brilliant blue R250, and entire gel lanes were cut in 20–25 slices. Each gel slice was further cut into 1 × 1–mm cubes and in-gel digested with trypsin as described in Shevchenko et al. (2006). In brief, gel pieces were rinsed with 200 µl of water, shrunk with 200 µl acetonitrile, destained by adding 100 µl of 100 mM ammonium bicarbonate followed by 200 µl acetonitrile, and finally shrunk with acetonitrile. Then, gel pieces were incubated overnight at 37°C in 13 ng/µl of modified trypsin (Promega) in 10 mM ammonium bicarbonate and 10% acetonitrile. Peptides were extracted with 50 µl of 5% formic acid and 50% acetonitrile, and pooled extracts were dried down in a vacuum centrifuge. Peptides were redissolved in 15 µl of 5% formic acid and analyzed by liquid chromatography tandem MS (LC MS/MS).

Protein identification by LC MS/MS

LC-MS/MS analysis was performed on an UltiMate 3000 Nano LC System (Dionex) interfaced online to a linear ion trap LTQ mass spectrometer (Thermo Fisher Scientific), as described in Shevchenko et al. (2008). The mobile phase was 0.1% formic acid in water (solvent A) and 100% of acetonitrile (solvent B). Peptide mixtures were separated using an 80-min gradient from 5 to 100% of solvent B. In the data-dependent acquisition cycle, the three most abundant precursor ions detected in the full MS survey scan (*m/z* range of 350–1,700) were isolated and fragmented. MS/MS fragmentation was triggered by a minimum signal intensity threshold of 500 counts. *m/z* of fragmented precursors was dynamically excluded for another 60 s. Acquired spectra were converted to Mascot generic format and then searched against *Drosophila* sequences in the National Center for Biotechnology Information protein databases by MASCOT software (v.2.4.04; Matrix Science) installed on a local server. Database searching settings were set as mass tolerance 2 and 0.5 Da for precursor and fragment ions, respectively. Variable modifications were set as propionamide (C), N-acetylation (protein N terminus), and oxidation (M). Enzyme settings were set as trypsin, with one missed cleavage allowed. All protein hits matching with at least two peptides having a peptide ion score >30 were then manually evaluated.

Preparation of heads and retinas and WB

Drosophila heads were collected on dry ice and mashed with a pestle before the addition of lysis buffer and further mashing. *Drosophila* retinas were dissected in ice-cold PBS before addition of SDS loading buffer and mashing with a pestle. Lysates were incubated on ice for 30 min and clarified by centrifugation. Supernatants were collected and boiled with standard SDS loading buffer and processed for SDS-PAGE and wet transfer using standard laboratory procedures.

Immunohistochemistry and rhodopsin-trafficking assay

Pupal and adult eyes were prepared as previously described (Richard et al., 2006a). In brief, adult heads were removed, bisected, and fixed immediately with 8% PFA, 15% picric acid, and 75 mM Pipes, pH 7.4, for 40 min at room temperature, washed with PBS, pH 7.2, and cryopreserved by incubation in 10% sucrose in PBS, pH 7.2, for 30 min at room temperature and then in 25% sucrose in PBS, pH 7.2, overnight at 4°C . Heads were then embedded in Richard-Allan Scientific Neg-50 (Thermo Fisher Scientific), and 10-µm sections were cut on a cryostat microtome (HM560; Thermo Fisher Scientific). Flies for Rh1-trafficking assay were raised from egg to adult on carotenoid-free medium (10% dry yeast, 10% sucrose, 0.02% cholesterol, and 2% agar). Flies were supplemented with crystalline all-trans-retinal (Sigma-Aldrich), kept in the dark for 2 d, pulsed with light using a CFP filter for 10 min, and then returned to the dark. Flies were fixed whole in the dark for 2 h in 8% PFA, 15% picric acid, and 75 mM Pipes, pH 7.4, and then processed as previously described. All images were acquired with a microscope (LSM510; Carl Zeiss) using a Plan-Apochromat 63× oil objective (1.4 NA; Carl Zeiss) and processed using Fiji and Photoshop (Adobe) software to adjust global brightness and contrast.

Quantification of MyoV fluorescence

Image processing was performed using Fiji. Total MyoV fluorescence levels were obtained from WT and *crb* mutant tissue, normalized first to the number of ommatidia, and then expressed as a function of MyoV levels in the WT tissue. SD was calculated using the mean ommatidium fluorescence as a function of WT levels between different fields of view.

EM

Eyes were prepared as in Tepass and Hartenstein (1994), with minor modifications. Eyes were fixed in 2.5% glutaraldehyde and 2.5% formaldehyde in 0.1 M phosphate buffer, pH 7.4, followed by fixation in 1% OsO_4/2% glutaraldehyde and then 2% OsO_4. After dehydration, eyes were embedded in Araldite, and 0.1-µm ultrathin sections were contrasted and analyzed with a Tecnai 12 BioTWIN (FEI Company) and photographed with a digital camera (F214A; TemCam).

S2R+ culture, transfection, and immunostaining

S2R+ cells were cultured in Schneider's medium (Sigma-Aldrich) supplemented with 10% FCS at 24°C. Transfection was performed using FuGene (Roche). Cells were plated onto concanavalin A–coated coverslips at 75,000 cells per well of a 24-well dish. After 24 h, cells were transfected by mixing 3 µl FuGene with 2 µg of plasmids (1 µg pActin5C-Gal4 and 1 µg pUASp-Crb/ pUASp-$Crb^{intramyc}$ [Klebes and Knust, 2000]/pUASp-Crb^{8F105}/pUASp-$Crb^{intramyc\Delta ERLI}$ [Klebes and Knust, 2000]/1 µg pUASp-MyoV-GFP or 0.5 µg of each for double transfection) in 100 µl Schneider's medium, which was distributed between 4 wells for quadruplicate coverslips. Cells were fixed 48 h after transfection with 4% PFA in PBS for 10 min. Fixed cells were washed with PBS, permeabilized with 0.1% Triton X-100 in PBS, blocked with 5% normal horse serum in blocking solution, and incubated with primary antibodies for 1 h at room temperature. Cells were washed with PBS, incubated with secondary antibodies for 1 h at room temperature, washed with PBS, and mounted onto glass slides using Mowiol and DABCO (Sigma-Aldrich). Imaging was performed on an upright microscope (710; Carl Zeiss) using a C-Apochromat 40× water objective (1.2 NA; Carl Zeiss). Images were processed using Fiji and Photoshop software to adjust global brightness and contrast.

Online supplemental material

Fig. S1 shows that Rh1 accumulates in the cell body of $MyoV^{Q105st}$ mutant photoreceptors and that 20-d-old w^- rhabdomeres do not degenerate. Fig. S2 shows that the rhabdomere terminal web is not disrupted in crb^{11A22} mutants. Fig. S3 shows Sdt localization in crb^{11A22} and crb^{8F105} mutant photoreceptors. Fig. S4 shows that Crb transgene expression in S2R+ cells does not induce Sdt expression. Online supplemental material is available at http://www.jcb.org/cgi/content/full/jcb.201105144/DC1.

We would like to thank D. Ready, A. Ephrussi, and the Bloomington Stock Center for flies, DNA constructs, and antibodies. We thank Katja Kapp for advice on S2R+ cells, Michaela Rentsch for help with EM, and Andrea Knaust for technical assistance with MS sample preparation and analysis. We are extremely grateful to Marta Luz and Thomas Wassmer for critically reading the manuscript. We also thank the Light Microscopy Facility of the Max Planck Institute of Molecular Cell Biology and Genetics, in particular P. Pitrone, for microscopy assistance.

This work was supported by the Max Planck Society and grants from the European Commission (HEALTH-F2-2008-200234) and Deutsche Forschungsgemeinschaft (Kn250/21-1) to E. Knust.

Submitted: 25 May 2011
Accepted: 27 October 2011

References

Alloway, P.G., L. Howard, and P.J. Dolph. 2000. The formation of stable rhodopsin-arrestin complexes induces apoptosis and photoreceptor cell degeneration. *Neuron*. 28:129–138. http://dx.doi.org/10.1016/S0896-6273(00)00091-X

Bachmann, A., M. Timmer, J. Sierralta, G. Pietrini, E.D. Gundelfinger, E. Knust, and U. Thomas. 2004. Cell type-specific recruitment of *Drosophila* Lin-7 to distinct MAGUK-based protein complexes defines novel roles for Sdt and Dlg-S97. *J. Cell Sci.* 117:1899–1909. http://dx.doi.org/10.1242/jcs.01029

Bachmann, A., F. Grawe, K. Johnson, and E. Knust. 2008. *Drosophila* Lin-7 is a component of the Crumbs complex in epithelia and photoreceptor cells and prevents light-induced retinal degeneration. *Eur. J. Cell Biol.* 87:123–136. http://dx.doi.org/10.1016/j.ejcb.2007.11.002

Belote, J.M., and E. Fortier. 2002. Targeted expression of dominant negative proteasome mutants in *Drosophila melanogaster*. *Genesis*. 34:80–82. http://dx.doi.org/10.1002/gene.10131

Berger, S., N.A. Bulgakova, F. Grawe, K. Johnson, and E. Knust. 2007. Unraveling the genetic complexity of *Drosophila* stardust during photoreceptor morphogenesis and prevention of light-induced degeneration. *Genetics*. 176:2189–2200. http://dx.doi.org/10.1534/genetics.107.071449

Borst, A. 2009. *Drosophila*'s view on insect vision. *Curr. Biol.* 19:R36–R47. http://dx.doi.org/10.1016/j.cub.2008.11.001

Bulgakova, N.A., and E. Knust. 2009. The Crumbs complex: From epithelial-cell polarity to retinal degeneration. *J. Cell Sci.* 122:2587–2596. http://dx.doi.org/10.1242/jcs.023648

Bulgakova, N.A., O. Kempkens, and E. Knust. 2008. Multiple domains of Stardust differentially mediate localisation of the Crumbs-Stardust complex during photoreceptor development in *Drosophila*. *J. Cell Sci.* 121:2018–2026. http://dx.doi.org/10.1242/jcs.031088

Chinchore, Y., A. Mitra, and P.J. Dolph. 2009. Accumulation of rhodopsin in late endosomes triggers photoreceptor cell degeneration. *PLoS Genet.* 5:e1000377. http://dx.doi.org/10.1371/journal.pgen.1000377

den Hollander, A.I., J. Davis, S.D. van der Velde-Visser, M.N. Zonneveld, C.O. Pierrottet, R.K. Koenekoop, U. Kellner, L.I. van den Born, J.R. Heckenlively, C.B. Hoyng, et al. 2004. CRB1 mutation spectrum in inherited retinal dystrophies. *Hum. Mutat.* 24:355–369. http://dx.doi.org/10.1002/humu.20093

den Hollander, A.I., R. Roepman, R.K. Koenekoop, and F.P.M. Cremers. 2008. Leber congenital amaurosis: Genes, proteins and disease mechanisms. *Prog. Retin. Eye Res.* 27:391–419. http://dx.doi.org/10.1016/j.preteyeres.2008.05.003

Grawe, F., A. Wodarz, B. Lee, E. Knust, and H. Skaer. 1996. The *Drosophila* genes crumbs and stardust are involved in the biogenesis of adherens junctions. *Development*. 122:951–959.

Griciuc, A., L. Aron, M.J. Roux, R. Klein, A. Giangrande, and M. Ueffing. 2010. Inactivation of VCP/ter94 suppresses retinal pathology caused by misfolded rhodopsin in *Drosophila*. *PLoS Genet.* 6:e1001075. http://dx.doi.org/10.1371/journal.pgen.1001075

Izaddoost, S., S.C. Nam, M.A. Bhat, H.J. Bellen, and K.W. Choi. 2002. *Drosophila* Crumbs is a positional cue in photoreceptor adherens junctions and rhabdomeres. *Nature*. 416:178–183. http://dx.doi.org/10.1038/nature720

Johnson, K., F. Grawe, N. Grzeschik, and E. Knust. 2002. *Drosophila* crumbs is required to inhibit light-induced photoreceptor degeneration. *Curr. Biol.* 12:1675–1680. http://dx.doi.org/10.1016/S0960-9822(02)01180-6

Kennan, A., A. Aherne, and P. Humphries. 2005. Light in retinitis pigmentosa. *Trends Genet.* 21:103–110. http://dx.doi.org/10.1016/j.tig.2004.12.001

Kiselev, A., M. Socolich, J. Vinós, R.W. Hardy, C.S. Zuker, and R. Ranganathan. 2000. A molecular pathway for light-dependent photoreceptor apoptosis in *Drosophila*. *Neuron*. 28:139–152. http://dx.doi.org/10.1016/S0896-6273(00)00092-1

Klebes, A., and E. Knust. 2000. A conserved motif in Crumbs is required for E-cadherin localisation and zonula adherens formation in *Drosophila*. *Curr. Biol.* 10:76–85. http://dx.doi.org/10.1016/S0960-9822(99)00277-8

Krauss, J., S. López de Quinto, C. Nüsslein-Volhard, and A. Ephrussi. 2009. Myosin-V regulates oskar mRNA localization in the *Drosophila* oocyte. *Curr. Biol.* 19:1058–1063. http://dx.doi.org/10.1016/j.cub.2009.04.062

Kumar, J.P., and D.F. Ready. 1995. Rhodopsin plays an essential structural role in *Drosophila* photoreceptor development. *Development*. 121:4359–4370.

Li, B.X., A.K. Satoh, and D.F. Ready. 2007. Myosin V, Rab11, and dRip11 direct apical secretion and cellular morphogenesis in developing *Drosophila* photoreceptors. *J. Cell Biol.* 177:659–669. http://dx.doi.org/10.1083/jcb.200610157

Nichols, R., and W.L. Pak. 1985. Characterization of *Drosophila melanogaster* rhodopsin. *J. Biol. Chem.* 260:12670–12674.

Pellikka, M., G. Tanentzapf, M. Pinto, C. Smith, C.J. McGlade, D.F. Ready, and U. Tepass. 2002. Crumbs, the *Drosophila* homologue of human CRB1/RP12, is essential for photoreceptor morphogenesis. *Nature*. 416:143–149. http://dx.doi.org/10.1038/nature721

Peng, Y.W., M. Zallocchi, W.M. Wang, D. Delimont, and D. Cosgrove. 2011. Moderate light-induced degeneration of rod photoreceptors with delayed transducin translocation in shaker1 mice. *Invest. Ophthalmol. Vis. Sci.* 52:6421–6427. http://dx.doi.org/10.1167/iovs.10-6557

Pocha, S.M., and G.O. Cory. 2009. WAVE2 is regulated by multiple phosphorylation events within its VCA domain. *Cell Motil. Cytoskeleton.* 66:36–47. http://dx.doi.org/10.1002/cm.20323

Richard, M., F. Grawe, and E. Knust. 2006a. DPATJ plays a role in retinal morphogenesis and protects against light-dependent degeneration of photoreceptor cells in the *Drosophila* eye. *Dev. Dyn.* 235:895–907. http://dx.doi.org/10.1002/dvdy.20595

Richard, M., R. Roepman, W.M. Aartsen, A.G. van Rossum, A.I. den Hollander, E. Knust, J. Wijnholds, and F.P. Cremers. 2006b. Towards understanding CRUMBS function in retinal dystrophies. *Hum. Mol. Genet.* 15(Spec No 2): R235–R243. http://dx.doi.org/10.1093/hmg/ddl195

Richard, M., N. Muschalik, F. Grawe, S. Ozüyaman, and E. Knust. 2009. A role for the extracellular domain of Crumbs in morphogenesis of *Drosophila* photoreceptor cells. *Eur. J. Cell Biol.* 88:765–777. http://dx.doi.org/10.1016/j.ejcb.2009.07.006

Rodionov, V.I., A.J. Hope, T.M. Svitkina, and G.G. Borisy. 1998. Functional coordination of microtubule-based and actin-based motility in melanophores. *Curr. Biol.* 8:165–168. http://dx.doi.org/10.1016/S0960-9822(98)70064-8

Rogers, S.L., and V.I. Gelfand. 1998. Myosin cooperates with microtubule motors during organelle transport in melanophores. *Curr. Biol.* 8:161–164. http://dx.doi.org/10.1016/S0960-9822(98)70063-6

Rosenbaum, E.E., R.C. Hardie, and N.J. Colley. 2006. Calnexin is essential for rhodopsin maturation, Ca2+ regulation, and photoreceptor cell survival. *Neuron*. 49:229–241. http://dx.doi.org/10.1016/j.neuron.2005.12.011

Satoh, A.K., and D.F. Ready. 2005. Arrestin1 mediates light-dependent rhodopsin endocytosis and cell survival. *Curr. Biol.* 15:1722–1733. http://dx.doi.org/10.1016/j.cub.2005.08.064

Satoh, A., F. Tokunaga, S. Kawamura, and K. Ozaki. 1997. In situ inhibition of vesicle transport and protein processing in the dominant negative Rab1 mutant of *Drosophila*. *J. Cell Sci.* 110:2943–2953.

Satoh, A.K., J.E. O'Tousa, K. Ozaki, and D.F. Ready. 2005. Rab11 mediates post-Golgi trafficking of rhodopsin to the photosensitive apical membrane of *Drosophila* photoreceptors. *Development*. 132:1487–1497. http://dx.doi.org/10.1242/dev.01704

Satoh, A.K., B.X. Li, H. Xia, and D.F. Ready. 2008. Calcium-activated Myosin V closes the *Drosophila* pupil. *Curr. Biol.* 18:951–955. http://dx.doi.org/10.1016/j.cub.2008.05.046

Shevchenko, A., H. Tomas, J. Havlis, J.V. Olsen, and M. Mann. 2006. In-gel digestion for mass spectrometric characterization of proteins and proteomes. *Nat. Protoc.* 1:2856–2860. http://dx.doi.org/10.1038/nprot.2006.468

Shevchenko, A., A. Roguev, D. Schaft, L. Buchanan, B. Habermann, C. Sakalar, H. Thomas, N.J. Krogan, A. Shevchenko, and A.F. Stewart. 2008. Chromatin Central: Towards the comparative proteome by accurate mapping of the yeast proteomic environment. *Genome Biol.* 9:R167. http://dx.doi.org/10.1186/gb-2008-9-11-r167

Tabuchi, K., K. Sawamoto, E. Suzuki, K. Ozaki, M. Sone, C. Hama, T. Tanifuji-Morimoto, Y. Yuasa, Y. Yoshihara, A. Nose, and H. Okano. 2000. GAL4/UAS-WGA system as a powerful tool for tracing *Drosophila* transsynaptic neural pathways. *J. Neurosci. Res.* 59:94–99. http://dx.doi.org/10.1002/(SICI)1097-4547(20000101)59:1<94::AID-JNR11>3.0.CO;2-Q

Tepass, U. 1996. Crumbs, a component of the apical membrane, is required for zonula adherens formation in primary epithelia of *Drosophila*. *Dev. Biol.* 177:217–225. http://dx.doi.org/10.1006/dbio.1996.0157

Tepass, U., and E. Knust. 1993. Crumbs and stardust act in a genetic pathway that controls the organization of epithelia in *Drosophila melanogaster*. *Dev. Biol.* 159:311–326. http://dx.doi.org/10.1006/dbio.1993.1243

Tepass, U., and V. Hartenstein. 1994. The development of cellular junctions in the *Drosophila* embryo. *Dev. Biol.* 161:563–596. http://dx.doi.org/10.1006/dbio.1994.1054

Tepass, U., C. Theres, and E. Knust. 1990. crumbs encodes an EGF-like protein expressed on apical membranes of *Drosophila* epithelial cells and required for organization of epithelia. *Cell*. 61:787–799. http://dx.doi.org/10.1016/0092-8674(90)90189-L

Wang, T., and C. Montell. 2007. Phototransduction and retinal degeneration in *Drosophila*. *Pflugers Arch.* 454:821–847. http://dx.doi.org/10.1007/s00424-007-0251-1

Wang, X., T. Wang, Y. Jiao, J. von Lintig, and C. Montell. 2010. Requirement for an enzymatic visual cycle in *Drosophila*. *Curr. Biol.* 20:93–102. http://dx.doi.org/10.1016/j.cub.2009.12.022

Wodarz, A., F. Grawe, and E. Knust. 1993. CRUMBS is involved in the control of apical protein targeting during *Drosophila* epithelial development. *Mech. Dev.* 44:175–187. http://dx.doi.org/10.1016/0925-4773(93)90066-7

Wodarz, A., U. Hinz, M. Engelbert, and E. Knust. 1995. Expression of crumbs confers apical character on plasma membrane domains of ectodermal epithelia of *Drosophila*. *Cell*. 82:67–76. http://dx.doi.org/10.1016/0092-8674(95)90053-5

Woolner, S., and W.M. Bement. 2009. Unconventional myosins acting unconventionally. *Trends Cell Biol.* 19:245–252. http://dx.doi.org/10.1016/j.tcb.2009.03.003

Xia, H., and D.F. Ready. 2011. Ectoplasm, ghost in the R cell machine? *Dev. Neurobiol.* In press.

Published November 21, 2011

Supplemental material

JCB

Pocha et al., http://www.jcb.org/cgi/content/full/jcb.201105144/DC1

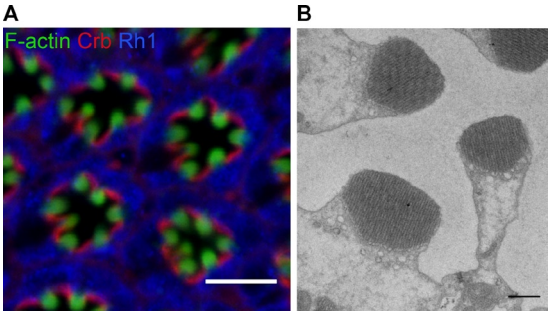

Figure S1. **Rh1 accumulates in the cell body of *MyoV*^{Q105st} mutant photoreceptors, and 20-d-old w^- rhabdomeres do not degenerate.** (A) Section through a *MyoV*^{Q105st} mutant retina stained for Rh1, Crb, and F-actin (to mark rhabdomeres). Bar, 5 µm. (B) Electron micrograph of w^- retina from 20-dpe adult flies showing no signs of degeneration. Bar, 1 µm.

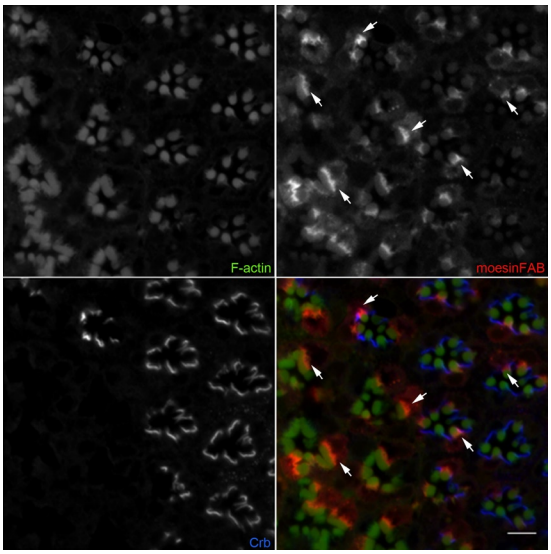

Figure S2. **The rhabdomere terminal web is not disrupted in *crb*^{11A22} mutants.** Section through an adult retina containing *crb*^{11A22} clones and expressing the UAS-moesin F-actin–binding domain GFP (moesinFAB) under the control of GMR-Gal4, stained for Crb, GFP, and F-actin. Arrows highlight moesin F-actin–binding localization to the F-actin tracks at the base of rhabdomeres in both WT and *crb* mutant. Bar, 5 µm.

Published November 21, 2011

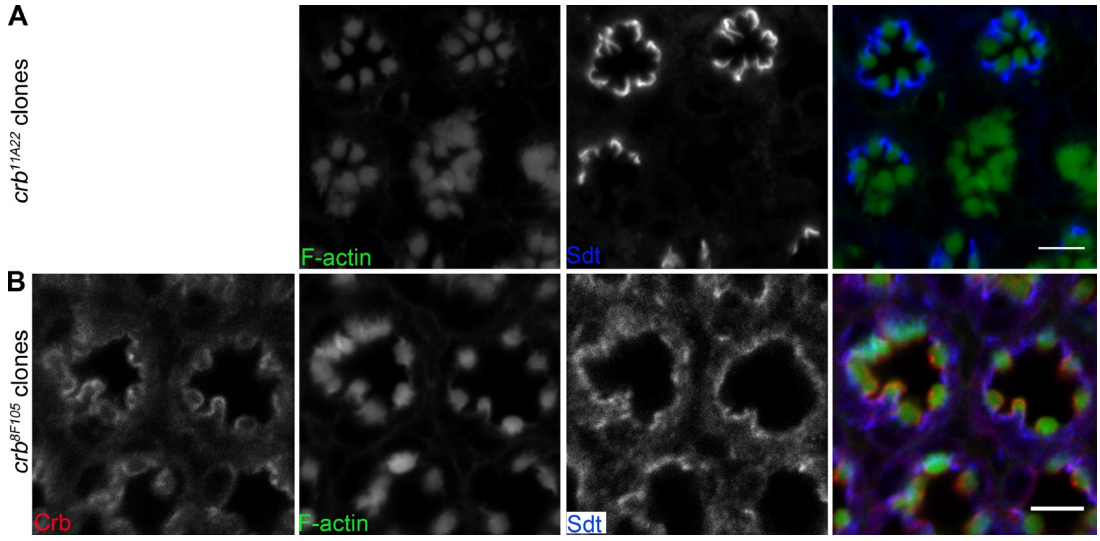

Figure S3. **Sdt localization in *crb*^{11A22} and *crb*^{8F105} mutant photoreceptors.** (A) Section through an adult retina containing *crb*^{11A22} clones and stained for F-actin and Sdt. (B) Section through an adult retina containing *crb*^{8F105} clones and stained for F-actin, Crb, and Sdt. Bars, 5 µm.

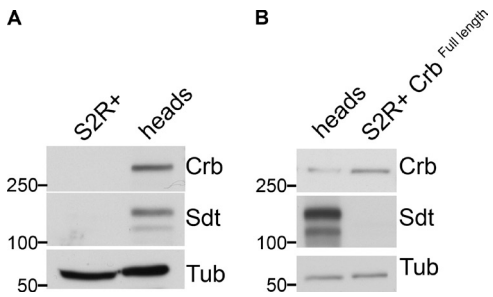

Figure S4. **Crb transgene expression in S2R+ cells does not induce Sdt expression.** (A and B) Western blots from WT adult *Drosophila* heads and whole-cell lysates of S2R+ cells (A) or S2R+ cells expressing full-length Crb and probed for Crb and Sdt, showing that neither is present in the S2R+ cells (A) and that Sdt expression is not induced upon Crb expression (B). Tubulin (Tub) is used as a loading control. The markers shown are for molecular masses in kilodaltons.